Catalysis Today xxx (xxxx) xxx–xxx

Contents lists available at ScienceDirect

Catalysis Today

journal homepage: www.elsevier.com/locate/cattod

Bimetallic Cu-based hollow fibre electrodes for CO_2 electroreduction

Ivan Merino-Garcia[a,*], Jonathan Albo[a], Piotr Krzywda[b], Guido Mul[b], Angel Irabien[a]

[a] Department of Chemical and Biomolecular Engineering, University of Cantabria, Avenida de los Castros s/n, 39005 Santander, Cantabria, Spain
[b] The PhotoCatalytic Synthesis (PCS) Group, MESA+ Institute for Nanotechnology, Faculty of Science and Technology, University of Twente, Enschede, 7500 AE, Netherlands

ARTICLE INFO

Keywords:
Electrochemistry
CO_2 electroconversion
Cu-based hollow fibre electrodes
Climate change

ABSTRACT

The electrochemical reduction of CO_2 represents an attractive alternative to both, i) satisfy the increasing energy demand, and ii) to help closing the carbon cycle. However, the energy required for CO_2 activation and the subsequent required multiple number of proton-coupled electron transfer steps, makes this process very challenging. Besides, catalytic material limitations hamper the application of this technology in the short term. Consequently, in this work we synthesise, characterise and preliminarily evaluate bimetallic Cu-based hollow fibre electrodes with a compact three-dimensional geometry to overcome mass transfer limitations and to enhance the electrochemical conversion of CO_2. The Cu hollow fibres are functionalised with Au in an attempt to tune the binding energy of the CO* intermediate, which appears to be key in the reduction of CO_2. The Cu fibres are also functionalised with Ni, aiming to decrease the reaction overpotential, resulting in beneficial energy efficiency. The so prepared Cu-based porous hollow fibre electrodes are obtained by dry-wet spinning and electrodeposition procedures. The materials are then characterised by scanning electron microscopy, energy dispersive X-ray spectroscopy, X-ray diffraction analyses and cyclic voltammetry. Finally, preliminary results of CO_2 electroreduction in a divided three-electrode cell are reported. The results show the potential of highly active, bimetallic hollow fibre-based electrocatalysts for enhanced conversion of CO_2 into value-added products. Deposition of particles should be performed with care, not to affect pore characteristics and thus mass transfer properties.

1. Introduction

The accumulation of carbon dioxide (CO_2) in the atmosphere is considered one of the most important challenges of the 21st century owing to its adverse impact on global warming [1]. Therefore, innovative strategies must be taken into consideration in order to palliate the consequences of climate change. In this context, the possibility to electrochemically convert CO_2 into value-added products while using renewable energy sources (e.g. solar or wind-based energies) is appealing, to store intermittent renewable energy in chemical bonds [2]. Furthermore, the continuous burning of fossil fuels for the synthesis of chemicals might be considerably reduced, owing to the electrochemical conversion of CO_2 into value-added products at room temperature, facilitating a closed carbon cycle. However, the high energy requirements for the activation of CO_2, the slow kinetics of the electrochemical reaction as well as the low production rates achieved limit the practical application of this technology in the short term [3].

Moreover, the availability of cheap, active, efficient, selective and stable electrocatalytic materials for CO_2 electrovalorisation is still limited [4]. In this regard, different electrocatalysts have been applied in CO_2 electroreduction processes [5], in which copper (Cu)-based surfaces are among the most studied materials because of their ability to perform the electrocatalytic conversion of CO_2 into fuels [6]. However, the reported productivities, selectivities and efficiencies are still far from practically feasbile [7]. In this respect, good adsorption and mass transfer properties are often the main features required for Cu-based electrodes to achieve an enhanced electrocatalytic conversion of CO_2. Moreover, the competitive hydrogen evolution reaction needs to be controlled, in order to improve the selectivity of the process [8].

In this context, the design of Cu-based hollow fibre (HF) electrodes is particularly appealing due to the multiple advantages that can be found in this kind of materials such as their porous and three-dimensional structure, which may improve the accessibility to catalytically active sites as well as its availability. Besides, the possibility of improving the diffusion of reactants and products represents an attractive opportunity for CO_2 electroreduction processes, since the hollow fibre can act as both a gas diffuser and electrocatalyst.

Furthermore, the combination of metals to prepare multimetallic

* Corresponding author.
E-mail address: merinoi@unican.es (I. Merino-Garcia).

https://doi.org/10.1016/j.cattod.2019.03.025
Received 31 October 2018; Received in revised form 18 February 2019; Accepted 10 March 2019

electrocatalysts appears to be an attractive approach. This provides the possibility of tuning the adsorption properties of intermediate species. In addition, the utilization of metals that bind specific reaction intermediates (i.e. CO*) may induce enhanced CO_2 electroreduction rates, because the binding energy of the intermediate may be tuned, which might affect reaction mechanisms and the reaction overpotential, among others [9]. Several researchers have also demonstrated that these alterations in the adsorption properties, when using different Cu-based bimetallic materials, also induce changes in the selectivity of the CO_2 reduction reaction [10,11]. Nevertheless, further work is needed to deepen the understanding of the influence of different parameters such as composition ratio, and particle size and morphology, among others [12].

Therefore, the aim of this work is to prepare, characterise and preliminary evaluate bimetallic Cu-based HFs electrodes to induce enhanced CO_2 electroreduction rates and Faraday Effciency (FE). The Cu HFs are functionalised with Au (i.e. Cu-Au HFs) and Ni (i.e. Cu-Ni HFs) in an attempt to improve the adsorption of reaction intermediates and to decrease the reaction overpotential. Thus, this study represents an innovative approach to evaluate the application of bimetallic three-dimensional Cu-based hollow fibre electrocatalysts for CO_2 electroconversion. The effect of the HFs composition (i.e. Cu, CuO, Cu-Au and Cu-Ni HFs) on the catalytic activity of the materials is then discussed. Finally, the most active Cu-based HF electrodes are evaluated in a cell in terms of FE, as a function of the applied potential (E). This study is expected to provide new insights for developing innovative working electrodes for CO_2 electroreduction processes.

2. Experimental details

The electrocatalytic Cu HFs are prepared according to the procedure developed by Kas et al. [4]. In brief, Cu powder (Skyspring nanomaterials, particle size = 1–2 μm; purity = 99%) as catalyst precursor, N-methylpyrrolidone (NMP, Sigma Aldrich, 99.5 wt%) as solvent, and polyetherimide (PEI, General Electric, Ultem 1000) as polymer are mixed with a weight percent of 71%, 22% and 7%, respectively. The catalyst precursor is first added to the NMP solution, followed by continuous agitation in an ultrasonic bath for 30 min. The addition of PEI is carried out afterwards and the resulting mixture is finally heated (at 60 °C) and stirred for, at least, 2 h. The solution is then stirred overnight and then vacuum is applied for approximately 1 h. The spinning process (spinneret with inner and outer diameters of 0.8 mm and 2 mm, respectively) is performed at room temperature using a stainless steel vessel. A coagulation bath is utilised to collect the fibres once the mixture is pressed through the spinneret while deionized water is pumped (30 ml min^{-1}) through the bore of the spinneret. The distance between the spinneret outlet and the coagulation bath level (i.e. air gap) is set at around 1 cm. The obtained Cu HFs are kept in the coagulation bath for 24 h in order to remove NMP traces and complete the phase inversion process. After the drying step at room temperature for 1 day, the fibres are thermally treated at 600 °C for 3 h in air (1 °C min^{-1}) to remove PEI as well as for Cu sintering, resulting in a porous CuO HF. Finally, the oxidised HFs are reduced by hydrogenation (4% H_2 in Ar) at 280 °C for 1 h, using a tube furnace.

The functionalisation of the Cu HFs is carried out through electrodeposition experiments in inert atmosphere while flowing N_2 gas through the hollow fibre. An undivided three-electrode cell (working electrode: Cu HF; counter electrode: Pt mesh; reference electrode: Ag/AgCl 3 M NaCl) is used to obtain the bimetallic electrocatalysts. A solution of $HAuCl_4$ (0.1 g/L) and 0.5 M H_2SO_4 (1:1 v/v) is used for Au electrodeposition at −0.9 V vs. Ag/AgCl for 10 min (current density of about 116 mA cm^{-2}). On the other hand, an aqueous solution 50 mM of $Ni(NO_3)_2{\cdot}6H_2O$ is used as electrolyte to functionalise Cu HFs with Ni at −1 V vs. Ag/AgCl for 15 min (current density of 2.5 mA cm^{-2}).

Different techniques were applied to physico-chemically characterise the catalytic materials. Scanning electron microscope (SEM) images were collected using a Zeiss Merlin HR-SEM with an acceleration voltage of 20 V–30 kV. X-ray diffraction (XRD) analyses were performed to evaluate the chemical composition of the materials using a Bruker D2 Phaser diffractometer, equipped with a Cu-Kα radiation source and operated at 30 kV and 10 mA. Besides, SEM-Energy dispersive X-ray spectroscopy (EDX) images were also collected. On the other hand, the electrochemical characterisation of the materials was carried out through cyclic voltammetry (CV) analyses using an undivided three-electrode cell, in which a Cu-based HF, a Pt wire and a Ag/AgCl-based electrode were applied as working, counter and reference electrodes, respectively. A CO_2-saturated 0.1 M $KHCO_3$ solution (pH 6.8) was used as electrolyte to fill the cell. A potential ranging from 1.5 V vs. Ag/AgCl to −1.5 V vs. Ag/AgCl with a voltage ramp of 20 mV s^{-1} was applied to the working electrode to analyse the electrochemical activity of each electrocatalytic material.

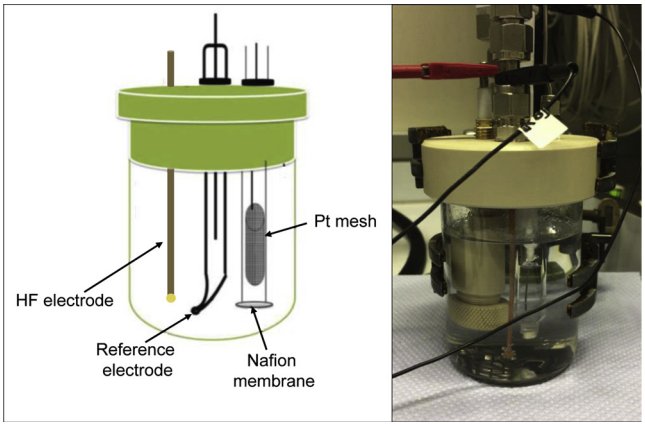

Fig. 1. Electrochemical cell.

The performance of the process was evaluated through preliminary CO_2 electroreduction experiments, which were conducted in a divided three-electrode cell (see Fig. 1), composed of the HF as working electrode (3.5 ± 0.5 cm), a Pt mesh as the counter electrode and a Ag/AgCl 3 M NaCl as the reference electrode. The CO_2 electroreduction experiments were performed at room temperature (20 °C). A Nafion 212 membrane divides the cell compartments, whereas a CO_2-saturated 0.1 M $KHCO_3$ solution was used as electrolyte. The hollow fibre electrode was connected to a stainless steel tube using conductive silver glue. Then, epoxy glue was applied on the top of silver glue to avoid the contact of the conductive silver glue with the electrolyte. The potentiostat clamp was then connected to the stainless steel tube. On the top of this tube, CO_2 was directly supplied into the fibre. The CO_2 flow rate was 20 ml min^{-1}, which flowed inside the material and was forced to cross the porous structure. For that purpose, the fibre was sealed at the bottom with epoxy glue. The influence of the applied potential was studied from −1.0 V vs. Ag/AgCl to −1.5 V vs. Ag/AgCl. It is worth noting that the reactor was purged with CO_2 (30 min) before measurements to saturate the electrolyte. The experiments were conducted for around 20 min, when steady state conditions were achieved. In addition, the reactor was also purged between potential changes. A gas chromatograph (GC) installed online, downstream of the cell and equipped with thermal conductivity detector (TCD), was used for the detection of H_2 and CO.

3. Results and discussion

3.1. Physico-chemical characterisation of the Cu-based HF electrodes

Fig. 2 shows different SEM images of the Cu HFs electrodes. The porous structure of the fibres is demonstrated in Fig. 2a–d, where voids can be clearly observed. Besides, Fig. 2c reveals that the sintering of Cu particles was successfully carried out and the Cu HFs show

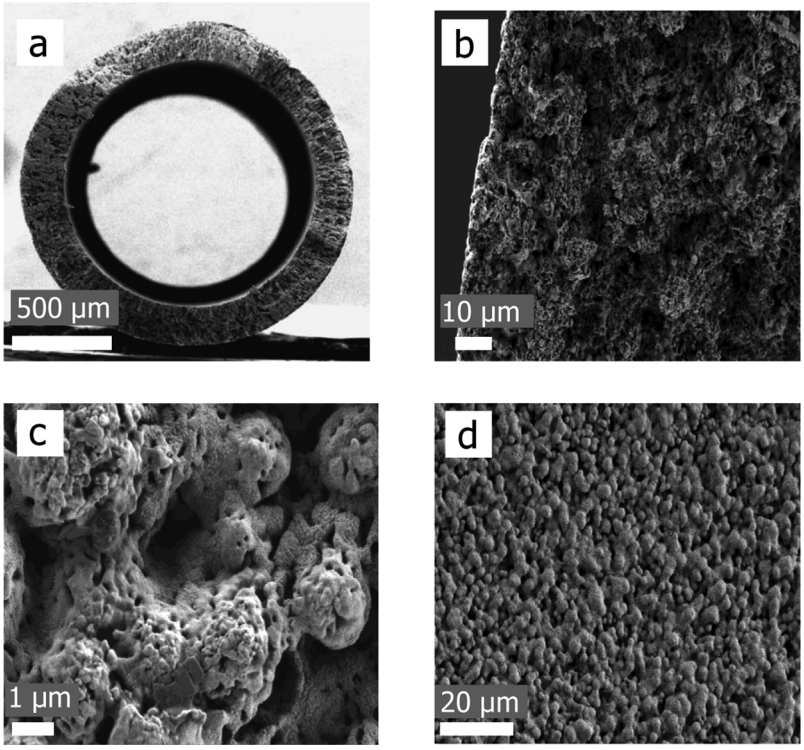

Fig. 2. SEM images of Cu HFs: a) [4] and b) Cross section, scale bars: 500 µm and 10 µm, respectively. c) External surface, scale bar :1 µm. d) Inner surface, scale bar :20 µm.

interconnected and aggregated Cu particles forming a three-dimensional porous structure. The so-prepared Cu HFs contain inner and outer diameters of approximately 1.3 mm and 1.6 mm, respectively (Fig. 2a). These porous three-dimensional structures might therefore enhance the accessibility of CO_2 to catalytically active sites, and also improve the diffusion of CO_2 in comparison with the use of two-dimensional working electrodes.

Fig. 3 displays the SEM images of the Cu-Au HFs, which provide evidence for the presence of Au clusters within the electrocatalytic material (bright areas), as well as the presence of oxides, which can be observed in Fig. 3c (black parts). Relatively fast oxidation of the Cu-Au HF apparently occurs in the presence of air. Overall, the electrodeposition of gold was successfully performed, even though further characterisation techniques need to be applied to confirm the formation of bimetallic Cu-Au particles.

Fig. 4 shows the SEM images of the Cu HFs electrodeposited with Ni. The presence of Ni as needle-like structures on the surface of the porous electrocatalyst can be clearly observed. The high porosity of the materials is remarkable, which may improve the diffusion of reactants and products through the wall of the fibre.

To further determine the composition of the Cu-based HF electrodes, different XRD measurements were carried out. Fig. 5 shows the XRD patterns for the different Cu materials obtained during the synthesis of Cu HFs (i.e. the calcined HF and the final reduced HF), including the Cu powder response. If we compare the resulting patterns, the same Cu crystal orientations can be clearly observed in both Cu powder and reduced HF (Cu 111, Cu 200 and Cu 220), which demonstrates the successful synthesis of this porous material. Besides, the presence of CuO is proven after the calcination step, which is converted into pure Cu after the reduction process.

The same procedure was followed to analyse the functionalised HF electrodes. Fig. 6 displays the XRD diagrams for Cu-Au HF (Fig. 6a, where the XRD pattern for Cu HF has been also included for comparison) and Cu-Ni HF (Fig. 6b). On the one hand, Fig. 6a reveals the presence of the Cu structures (Cu 111, Cu 200 and Cu 220) identified in the Cu HF, as well as four specific Au crystal orientations (Au 111, Au 200, Au 220 and Au 311), which confirms the presence of gold in the functionalised HF electrodes. On the other hand, Fig. 6b shows that the XRD response of Cu and Ni is practically equal in terms of diffraction angle. Therefore, the utilisation of other characterisation techniques is needed to demonstrate that the material is composed by Cu and Ni. Consequently, an EDX analysis (Fig. 7) of the outer surface of the Cu-Ni HF was carried out, demonstrating the presence of both Cu and Ni structures. Overall, XRD and EDX analyses demonstrate that the electrodeposition was successful.

3.2. Electrochemical characterisation of the Cu-based HF electrodes in the presence of CO_2

Fig. 8 shows the current-voltage responses for the materials (i.e. Cu, CuO, Cu-Au and Cu-Ni HFs electrodes). The calcined HFs (CuO) reach an unnoticeable current-voltage response compared to those voltammograms obtained for the reduced (Cu HFs) and functionalised fibre electrodes (Cu-Au and Cu-Ni HFs), which might be related to lack of conductivity of the fibre after the calcination step [13]. If we analyse the voltammetric profiles of the most active electrocatalytic materials (i.e. Cu HF and bimetallic HF), it can be seen that the highest response at −1.5 V vs. Ag/AgCl is achieved for the Cu HF electrodes, which might be initially related to reduction of surface oxides, followed by an enhanced production of H_2 and CO (syngas) as reported by Kas et al. [4], who previously electroreduced CO_2 to syngas at low applied potentials using Cu HFs electrodes. The lower current densities observed for the bimetallic HF electrodes can be associated with the electrodeposition procedures used for the synthesis of the Cu-Au and Cu-Ni bimetallic fibres. It is plausible to assume the copper oxide has been reduced at the negative potentials applied for the deposition of Ni and Au. The lower current densities observed in the range of −1.0 V to −1.5 V vs. Ag/AgCl could be due to differences in resistance, or pore dimensions, creating *sub*-optimal supply of CO_2. Kas et al. [4] have previously demonstrated that the current density is a function of CO_2

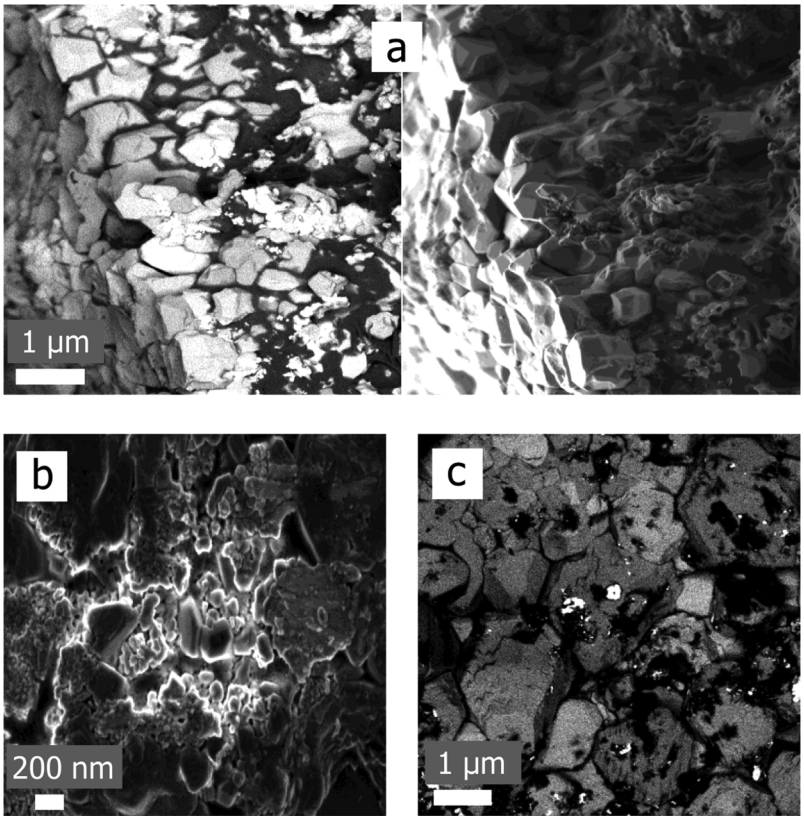

Fig. 3. SEM images of Cu-Au HFs: a) Cross section, scale bar = 1 µm. b) External surface, scale bar = 200 nm. c) Inner surface, scale bar = 1 µm.

flow rate and supply.

3.3. Preliminary CO_2 electroreduction experiments in cell

In order to evaluate the effect of Au and Ni on the reaction selectivity, four types of HF electrodes synthesised in this study (i.e. CuO, Cu, Cu-Au and Cu-Ni HFs) were evaluated at a potential ranging from −1.0 V to −1.5 V vs. Ag/AgCl. The results are shown in Table 1. It is important to point out that the use of CuO HF does not lead to any CO_2 reduction product, which is in accordance with the low current-voltage response observed in the CV analyses of Fig. 8.

The preliminary results suggest that the optimal potential range for the production of CO is from −1.25 V to −1.5 V vs. Ag/AgCl. An improved FE to CO can be observed with Cu-Ni HF at −1.25 V and −1.5 V vs. Ag/AgCl, including a higher current density level compared to those values obtained for Cu and Cu-Au HF electrodes, which may indicate the proton assisted electron transfer to CO_2 is promoted by the presence of Ni particles on the Cu HFs. This is in agreement with the lower FE

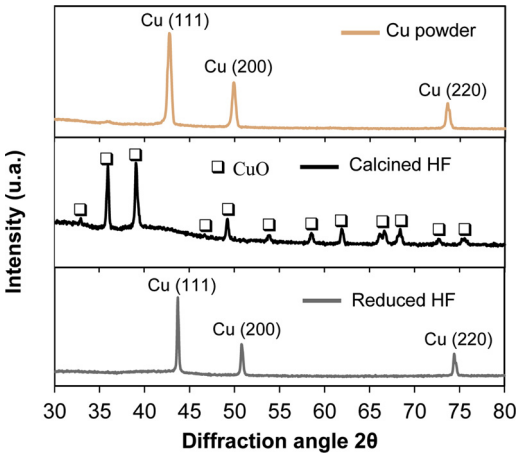

Fig. 5. XRD patterns for Cu powder, calcined HF and reduced HF.

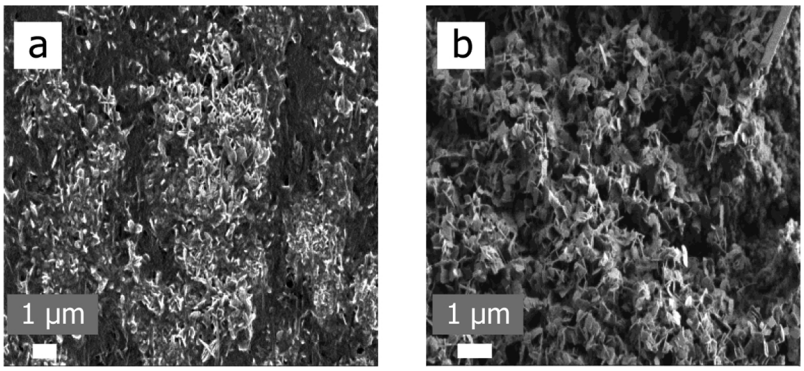

Fig. 4. SEM images of Cu-Ni HFs: a) External surface, scale bar = 1 µm. b) Inner surface, scale bar = 1 µm.

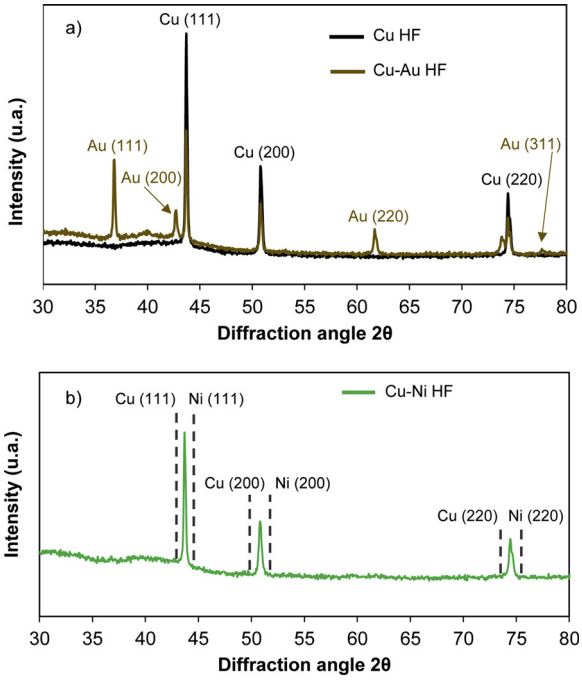

Fig. 6. XRD patterns for a) Cu-Au HF and b) Cu-Ni HF.

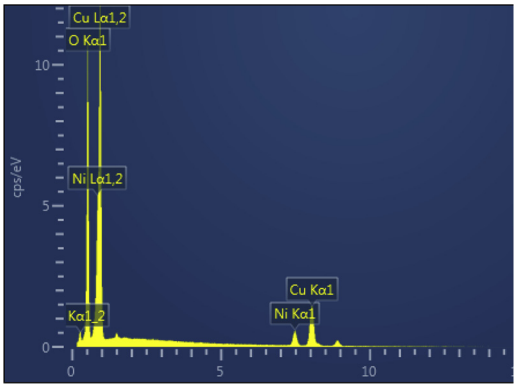

Fig. 7. EDX analysis of the Cu-Ni HF outer surface.

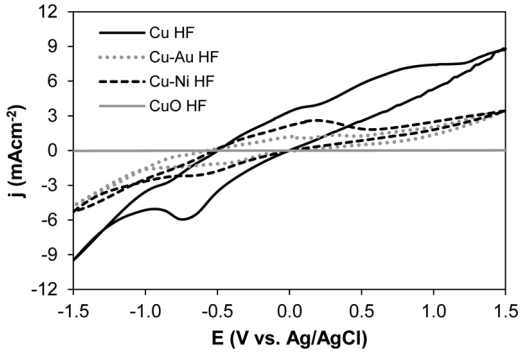

Fig. 8. CVs for Cu HF (black line), CuO HF (grey line), Cu-Au HF (grey dotted line) and Cu-Ni HF (black dotted line). The CVs were recorded in a CO_2-saturated 0.1 M $KCHO_3$ aqueous solution (For interpretation of the references to colour in this figure legend, the reader is referred to the web version of this article).

towards hydrogen in the presence of Ni at −1.25 V and −1.5 V. The FE does not close to 100%: the formation of formate and alcohols is very likely, and should account for the missing percentage. Analysis of formate and alcohols is presently performed to further characterise the behaviour of bimetallic hollow fibres. On the contrary, the utilisation of Cu-Au HF electrodes presents similar results in terms of FE to those reached at Cu HF electrodes, although the overall current density is lower. This might again be due to the plate-like, and irregular deposition of Au, which might reduce the number of effective pores through which CO_2 is provided to the reactive interface of Cu(Au), CO_2, and electrolyte. Moreover, the obtained current density values, especially for Cu-Ni HF at −1.5 V vs. Ag/AgCl (13.6 $mAcm^{-2}$), are of relevance when compared to previous reports on the electrochemical conversion of CO_2 at Cu-based electrodes. For instance, a current density ranging from 0.7 $mAcm^{-2}$ to 7.5 $mAcm^{-2}$ (as a function of different applied potential) was obtained for CO_2 electroreduction at Cu-based gas diffusion electrodes [14]. Besides, different Cu-based solid polymer electrolytes were applied in a membrane electrode assembly configuration for CO_2 electroconversion, where current densities ranged from 3.3 $mAcm^{-2}$ to 11.1 $mAcm^{-2}$ [15]. The innovative materials developed in the present study allow working at applied potentials ranging from −1 V to −1.5 V vs. Ag/AgCl, which are lower than those required for CO_2 electroconversion at Cu-based surfaces such as Cu nanoparticles and Cu nanofoams with applied voltages of −2.0 V vs. Ag/AgCl [14], −2.2 V vs. Ag/AgCl [16] and −1.7 V vs. Ag/AgCl [17], respectively. This denotes the interest in further developing hollow fibre electrode configurations for an improved CO_2 conversion with a higher energy efficiency.

In short, the preliminary results show differences in performance as compared to fibres made entirely out of copper. The advantages observed in terms of FE to CO, and enhanced current density when using Cu-Ni HF electrodes can likely be associated with a synergic effect between Cu and Ni in the CO_2 conversion pathway. However, further work is required to improve the performance of the deposition process of metallic particles on the copper fibres, with focus on control of size and distribution of particles, and study of the effect of changes in the pore dimensions and associated gas flow characteristics on performance.

4. Conclusions

This study reports the synthesis, characterisation and preliminary evaluation of innovative electrode materials for the electroreduction of CO_2. Cu-based hollow fibre electrodes were prepared with a porous and three-dimensional geometry, acting as both gas diffusers and working electrodes. These materials were then functionalised with Au and Ni through electrodeposition experiments to obtain bimetallic hollow fibre electrodes with potential to enhance the electroconversion of CO_2.

SEM images show the well-defined porous structure of the materials. Besides, the bimetallic Cu-Au and Cu-Ni hollow fibre images demonstrate the presence of Au and Ni in the form of clusters and needles, respectively. Deposition was further characterised by XRD and EDX analyses. Cyclic voltammetry analyses reveal a promising catalytic activity of Cu, Cu-Au and Cu-Ni HFs. The differences in activity at −1.5 V vs. Ag/AgCl might be related to changes in reaction mechanisms owing to the presence of metallic components, while for Au inferior pore characteristics and associated inferior mass transfer properties might be the cause of lower current densities. The preliminary CO_2 electroreduction experiments show enhanced FE to CO and improved current density using Cu-Au and Cu-Ni hollow fibres in comparison to those results obtained when the fibre is based on pure Cu. Nevertheless, further studies should be carried out to enhance the performance of the fibres.

Overall, this research work should be of help for developing active and efficient electrocatalytic materials for CO_2 electro-valorisation processes.

Table 1
FE results from CO_2 electroreduction at Cu–based HF electrodes as a function of the applied potential.

Electrocatalyst	E = −1.0 V			E = −1.25 V			E = −1.5 V		
	FE (%)		j ($mAcm^{-2}$)	FE (%)		j ($mAcm^{-2}$)	FE (%)		j ($mAcm^{-2}$)
	CO	H_2		CO	H_2		CO	H_2	
Cu HF	43.2	11.3	2.2	66.1	8.6	6.6	63.2	11.8	12.7
Cu-Au HF	27.8	9.7	1.8	64.7	10.7	4.3	67.2	12.9	8.0
Cu-Ni HF	45.7	39.6	2.2	76.3	7.4	6.8	77.5	9.3	13.6

Acknowledgements

I. M-G would like to thank the Spanish Ministry of Economy and Competitiveness (MINECO) for the Early Stage Researcher Contract, including the Research Stay grant (EEBB-I-17-12382) as well as the postdoctoral period of the predoctoral contract (BES-2014-070081). I. M-G, J. A and A. I gratefully acknowledge financial support from the MINECO through the projects CTQ2013-48280-C3-1-R and CTQ2016-76231-C2-1-R, as well as Ramón y Cajal programme (RYC-2015-17080). G. M also acknowledges NanoNextNL, a micro and nano-technology consortium of the Government of the Netherlands and 130 partners.

References

[1] C. Dong, X. Dong, Q. Jiang, K. Dong, G. Liu, Sci. Total Environ. 622–623 (2018) 1294–1303.
[2] I. Merino-Garcia, E. Alvarez-Guerra, J. Albo, A. Irabien, Chem. Eng. J. 305 (2016) 104–120.
[3] H.R.M. Jhong, S. Ma, P.J.A. Kenis, Curr. Opin. Chem. Eng. 2 (2013) 191–199.
[4] R. Kas, K.K. Hummadi, R. Kortlever, P. de Wit, A. Milbrat, M.W.J. Luiten-Olieman, N.E. Benes, M.T.M. Koper, G. Mul, Nat. Commun. 7 (2016) 10748.
[5] J. Qiao, Y. Liu, F. Hong, J. Zhang, Chem. Soc. Rev. 43 (2014) 631–675.
[6] A.A. Peterson, F. Abild-Pedersen, F. Studt, J. Rossmeisl, K. Nørskov, Energy Environ. Sci. 3 (2010) 1311–1315.
[7] I. Merino-Garcia, J. Albo, A. Irabien, Nanotechnology 29 (2018) 014001.
[8] D.W. Dewulf, A.J. Bard, Catal. Lett. 1 (1988) 73–80.
[9] R. Kortlever, I. Peters, C. Balemans, R. Kas, Y. Kwon, G. Mul, M.T.M. Koper, Chem. Commun. 52 (2016) 10229–10232.
[10] J.T. Billy, A.C. Co, Appl. Catal. B-Environ. 237 (2018) 911–918.
[11] Z. Chang, S. Huo, W. Zhang, J. Fang, H. Wang, J. Phys. Chem. C 121 (2017) 11368–11379.
[12] C.W. Lee, K.D. Yang, D.-H. Nam, J.H. Jang, N.H. Cho, S.W. Im, K.T. Nam, Adv. Mater. (2018) 1704717.
[13] O. Amadine, Y. Essamlali, A. Fihri, M. Larzek, M. Zahouily, RSC Adv. 7 (2017) 12586–12597.
[14] I. Merino-Garcia, J. Albo, A. Irabien, Energy Technol. 5 (2017) 922–928.
[15] L.M. Aeshala, S.U. Rahman, A. Verma, Sep. Purif. Technol. 94 (2012) 131–137.
[16] O.A. Baturina, Q. Lu, M.A. Padilla, L. Xin, W. Li, A. Serov, K. Artyushkova, P. Atanassov, F. Xu, A. Epshteyn, T. Brintlinger, M. Schuette, G.E. Collins, ACS Catal. 4 (2014) 3682–3695.
[17] S. Sen, D. Liu, G.T.R. Palmore, ACS Catal. 4 (2014) 3091–3095.